

Note

Solution conformation and dynamics of a tetrasaccharide related to the Lewis^X antigen deduced by ¹H NMR NOESY, ROESY, and T-ROESY measurements

Ana Poveda ^a, Juan Luis Asensio ^b, Manuel Martín-Pastor ^b,
Jesús Jiménez-Barbero ^{b,*}

^a *Servicio Interdepartamental de Investigación, Universidad Autónoma de Madrid, Cantoblanco, 28049 Madrid, Spain*

^b *Grupo de Carbohidratos, Instituto de Química Orgánica, C.S.I.C., Juan de la Cierva 3, 28006 Madrid, Spain*

Received 2 November 1996; accepted 24 January 1997

Abstract

The conformational and dynamical features of a Le^X tetrasaccharide analogue GalNAc(α1-3)Gal(β1-4)[Fuc(α1-3)]Glc(βOMe) **1** have been studied through ¹H NMR relaxation measurements. The results indicate that the different glycosidic linkages of **1** present distinct conformational flexibility in solution. In addition, the use of T-ROESY experiments in conformational analysis of oligosaccharides is explored emphasizing its scope and limitations. © 1997 Elsevier Science Ltd.

Keywords: Relaxation; Dynamics; Tetrasaccharide; T-ROESY; Internal motions

1. Introduction

The three-dimensional structure of carbohydrates is of primary importance for their involvement in biological recognition events [1,2]. There have been many reports in the last few years on the extent and nature of motion around the glycosidic linkages of oligosaccharides [3a,3b], regarding the existence of either constrained conformations [4] or conformational averaging [5] for different, or even the same,

carbohydrate structures. At the present moment, it is obvious that complete rigidity may be discarded. However, the ways of looking at the concept of flexibility are rather subjective and may range from the consideration of small torsional oscillations around a given conformer to the recognition of the simultaneous presence of two or more significantly different geometries. Up to now, indication of internal motion around glycosidic linkages has been directly obtained in small sugars as sucrose [6] and in other saccharides [3a,3b,7], and, very recently, evidence of the existence of flexibility in branched oligosaccharides has also been reported [8]. Moreover, recent investigations have postulated that the rates of global and

* Corresponding author. Fax: +34-1-5644853; e-mail: IQOJJ01@PINAR1.CSIC.ES.

internal motions of small to medium-size carbohydrates take place in similar timescales [3a,3b,4–9].

The conformation of the Le^X oligosaccharide and related structures has been a topic of interest during the past few years due to their direct implication in inflammatory and adhesion processes [10]. The reported results indicate that, in all the studied compounds, the branched Le^X trisaccharide moiety, $\text{Gal}(\beta 1-4)[\text{Fuc}(\alpha 1-3)]\text{GlcNAc}$, is rather rigid or just presents limited torsional oscillations around the glycosidic linkages [10]. It has been reported recently that a related compound, namely, $\text{GalNAc}(\alpha 1-3)\text{Gal}(\beta 1-4)[\text{Fuc}(\alpha 1-3)]\text{Glc}(\beta \text{OMe})$ **1**, shows inhibitory activity against the proliferation of astrocytes and transformed neural cell lines [11,12].

We now report on the application of ^1H NMR relaxation measurements to unequivocally characterise that, in contrast with common belief, a Le^X tetrasaccharide analogue, **1**, presents distinct conformational flexibility for the different glycosidic linkages in solution. In addition, we would like to stress the use of T-ROESY experiments [13] as a direct and useful tool in conformational analysis of oligosaccharides, and we here emphasize its scope and limitations depending on the molecular size (more precisely, global correlation time) of the oligosaccharide molecule.

2. Results and discussion

Intra- and inter-residue NOEs were obtained for the tetrasaccharide (Fig. 1) through 1D-NOESY (five mixing times between 100 and 800 ms, Fig. 2), 1D-T-ROESY (four mixing times between 100 and 400 ms), and 1D-ROESY (four mixing times between 100 and 400 ms) experiments at 299 K and 500 MHz. Cross-relaxation rates (σ_{ROE} , $\sigma_{\text{T-ROE}}$, σ_{NOE}) were obtained (see supplementary material) from these measurements [6]. A first attempt to characterize the

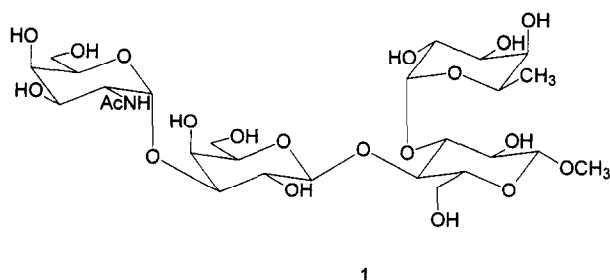


Fig. 1. Schematic view of tetrasaccharide **1**, showing the atomic numbering.

presence of fast internal motions was performed by obtaining $\sigma_{\text{ROE}}/\sigma_{\text{NOE}}$, $\sigma_{\text{T-ROE}}/\sigma_{\text{NOE}}$, and $\sigma_{\text{ROE}}/\sigma_{\text{T-ROE}}$ ratios (Fig. 3), since they allow to estimate specific correlation times [14] (Table 1) and, thus, interproton distances. There are small but significant differences between these ratios. In all cases, it can be observed that the obtained correlation times for proton pairs belonging to either the Gal or the Glc residues are higher than those within the Fuc and GalNAc rings. Therefore, according to the experimental results and, unexpectedly, the $\text{Fuc}(\alpha 1-3)\text{Glc}$ glycosidic linkage is as flexible as the terminal $\text{GalNAc}(\alpha 1-3)\text{Gal}$ analogue. The derived correlation times were used to estimate ranges of experimental distances which were compared to those deduced by molecular mechanics calculations.

In a second step, a more quantitative approach was performed by following a protocol based on that described by Lommersee et al. [15] (see also the experimental section). In this case, effective correlation times for specific proton pairs were calculated from the simultaneous evaluation of all (NOESY, ROESY, T-ROESY) proton–proton relaxation data obtained at 299 K. Interproton distances were estimated from molecular mechanics calculations. A fit of the experimental data to those calculated for different simplifications of the model-free approach described by Lipari and Szabo [16] allowed estimation of the relevant local correlation times. Intraresidue proton pairs were first evaluated, since they are basically independent of the conformation around the glycosidic linkages. The goodness of the fit was evaluated by using a residual factor [17], R_w (see experimental section).

Two facts are evident from this analysis (Table 2): In all cases, the residual factor, R_w , decreases with increasing complexity of the spectral density function, thus indicating that the explicit consideration of torsional flexibility around the glycosidic linkages indeed increases the fit between theoretical and observed data. Additionally, the obtained local correlation times for proton pairs within the Glc or Gal rings are always higher than those belonging to the Fuc or GalNAc moieties. This fact is again an indication of distinct flexibility for these two rings when compared to the lactose [$\text{Gal}(\beta 1-4)\text{Glc}$] moiety, as can also be deduced from the more qualitative analysis described before. Finally, the goodness of the fit was evaluated for the interresidue proton pairs (Table 3). Again, and as stated for the intraresidue proton pairs, the best fit (smaller R_w) is obtained when model III, with explicit consideration of different proton–proton local

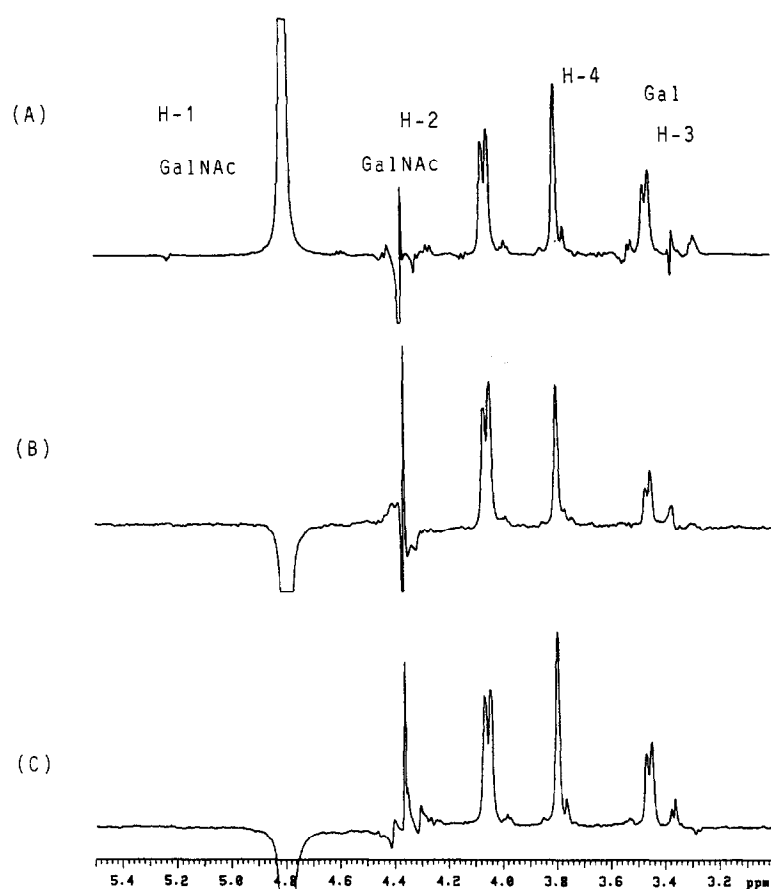


Fig. 2. Examples of selective one-dimensional (1D) experiments at 299 K to measure 500-MHz NOE effects for GalNAc H-1. From top to bottom, (A) 1D-NOESY (300 ms), (B) 1D-ROESY (200 ms), (C) 1D-T-ROESY (300 ms). The relevant intrasidue H-2 and interresidue Gal H-3 and Gal H-4 enhancements are marked.

correlation times [15], is employed. Isotropic motion was assumed in the analysis, since no major anisotropy is to be expected for this branched tetrasaccharide [18].

The existence of distinct flexibility for the different glycosidic linkages of this tetrasaccharide is in partial disagreement with previous results [10] for several analogues of **1**. The reported conclusions

Table 1

Relevant intra- and inter-residue proton-proton correlation times (τ_c , ns) estimated at 299 K from $\sigma_{\text{NOE}}/\sigma_{\text{ROE}}$, $\sigma_{\text{NOE}}/\sigma_{\text{T-ROE}}$, and $\sigma_{\text{ROE}}/\sigma_{\text{T-ROE}}$ ratios. Estimated errors are smaller than 15%

Proton pair	Correlation time τ_c (ns)	Proton pair	Correlation time τ_c (ns)
<i>Intrasidue peaks</i>			
Gal H-1/Gal H-3	1450	GalNAc H-1/GalNAc H-2	1010
Gal H-1/Gal H-2	1450	Average GalNAc	1010
Gal H-1/Gal H-5	1700	Fuc H-1/Fuc H-2	990
Average Gal	1550	Fuc H-5/Fuc H-3	870
Glc H-1/Glc H-5	1400	Fuc H-1/Fuc H-5	830
Glc H-1/Glc H-3	1650	Fuc H-5/Fuc H-4	950
Average Glc	1525	Average Fuc	890
<i>Interresidue peaks</i>			
Gal H-1/Glc H-4	1400	Gal H-1/Glc H-6	1100
GalNAc H-1/Gal H-3	900	GalNAc H-1/Gal H-4	950
Fuc H-1/Glc H-3	950	Fuc H-1/Glc H-2	700
Fuc H-5/Gal H-2	850		

Table 2

Motional parameters for different residues of the tetrasaccharide obtained at 299 K from least-squares fitting of the 500-MHz intrasidue experimental NOESY, ROESY, and T-ROESY cross-relaxation rates. The following intrasidue proton pairs were used: Gal H-1/Gal H-2, Gal H-1/Gal H-3, Gal H-1/Gal H-5, Glc H-1/Glc H-3, Glc H-1/Glc H-5, GalNAc H-1/GalNAc H-2, Fuc H-1/Fuc H-2, Fuc H-1/Fuc H-5, Fuc H-5/Fuc H-3, and Fuc H-5/Fuc H-4

Residue	Model	τ_{global} (ps)	$\tau_{\text{effective}}$ (ps)	R_w
Gal	I	1193		0.168
	III		1548	0.048
Glc	III		1318	0.048
GalNAc	III		1101	0.048
Fuc	III		968	0.048

were based mainly on the qualitative or semiquantitative analysis of the Fuc H-2/Gal H-2 NOE. In several cases, either hard-sphere or in-vacuo MD simulations were also performed. With these calculations, a strong stabilising interaction between the non-polar surfaces of the Fuc and Gal moieties is evident. Apart from this fact, which obviously overemphasises the existence of constrained conformations, these stacked structures are also favoured because of the heavy importance of the exo-anomeric term in the corresponding force fields [10]. Nevertheless, it has to be mentioned that, very recently, a Fuc(α 1-3)GlcNAc glycosidic linkage within a glycopeptide [15] has also been shown to be rather flexible, in agreement with our observations.

Regarding the use of T-ROESY experiments [13] (see experimental part for details) for extracting conformational information on oligosaccharide structures, different conclusions may be inferred from the dependence of $\sigma_{\text{T-ROE}}$ with the global correlation time and with the order parameter of the proton–proton vectors (Figs. 3 and 4).

Table 3

Motional parameters for different interresidue proton pairs of the tetrasaccharide obtained at 299 K from least-squares fitting of the 500-MHz experimental NOESY, ROESY, and T-ROESY cross-relaxation rates, and using the parameters derived for the intrasidue proton pairs. Experimental and molecular mechanics (MM) estimated distances (Å) are also given

Proton pair	Model	R_w	Distance _{exp} (Å)	Distance _{MM} (Å)
Gal H-1/Glc H-4	I	0.393	2.2–2.4	2.5
Gal H-1/Glc H-6	III	0.235	2.8–3.0	2.8
GalNAc H-1/Gal H-3	III	0.235	2.6–2.8	2.6
GalNAc H-1/Gal H-4	III	0.235	2.4–2.6	2.5
Fuc H-1/Glc H-3	III	0.235	2.2–2.4	2.6
Fuc H-1/Glc H-2	III	0.235	3.0–3.2	3.5
Fuc H-5/Gal H-2	III	0.235	2.6–2.8	2.6

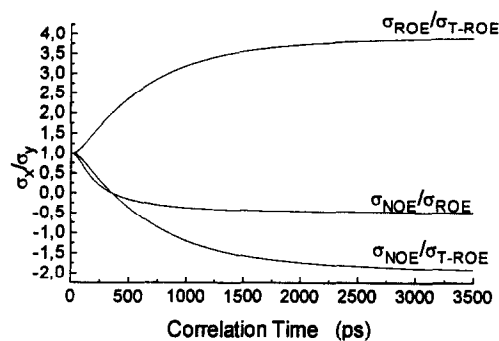


Fig. 3. Plot of the variation of 500-MHz $\sigma_{\text{NOE}}/\sigma_{\text{ROE}}$, $\sigma_{\text{NOE}}/\sigma_{\text{T-ROE}}$, and $\sigma_{\text{ROE}}/\sigma_{\text{T-ROE}}$ ratios with the correlation time of the corresponding proton pair under consideration. The results are independent of the models I–IV (see text) employed.

It is true that the use of T-ROESY permits the minimisation of the presence of spurious Hartmann–Hahn artifacts [19], which are always of major concern when ROESY spectra [20] of oligosaccharide molecules are recorded. This is clearly a major goal of this technique. Nevertheless, it has to be considered that $\sigma_{\text{T-ROE}}$ is, in fact, a linear combination [13] of σ_{ROE} and σ_{NOE} . Therefore, for molecules larger than that studied here (for instance, polysaccharides), its absolute value will be significantly smaller than that of σ_{ROE} , due to the opposite signs of σ_{ROE} and σ_{NOE} and, thus, partial cancellation of both quantities. In those cases, much more spectrometer time may be necessary to obtain an adequate signal/noise ratio in T-ROESY experiments for quantitative purposes. Nevertheless, for small and medium-size oligosaccharides, the use of T-ROESY may be the method of choice, as can be deduced from its correlation time-dependence shown in Figs. 3 and 4. It can be observed that the absolute value and the range of variation of the $\sigma_{\text{NOE}}/\sigma_{\text{T-ROE}}$ ratio are higher than that of the $\sigma_{\text{NOE}}/\sigma_{\text{ROE}}$ one, and seem particularly

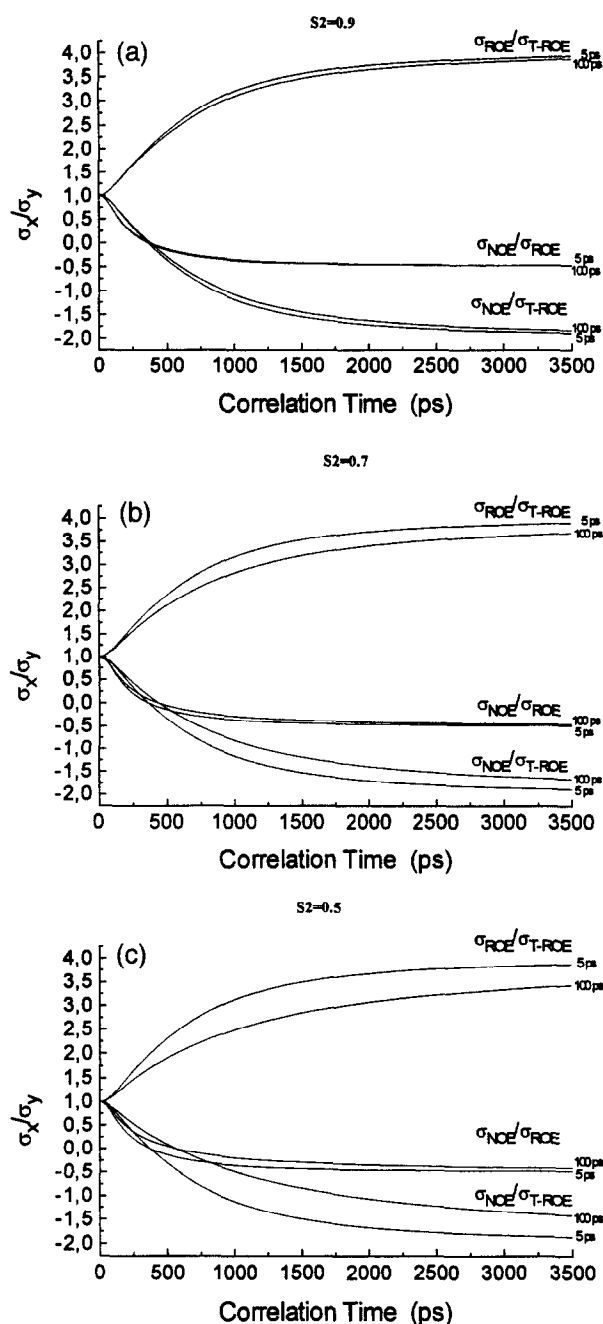


Fig. 4. Plot of the variation of 500-MHz $\sigma_{NOE}/\sigma_{ROE}$, $\sigma_{NOE}/\sigma_{T-ROE}$, and $\sigma_{ROE}/\sigma_{T-ROE}$ ratios with the correlation time of the corresponding proton pair under consideration under assumption of the Lipari–Szabo spectral density function (model V). (a) Results for order parameter S^2 0.9 and two fast internal correlation times of 5 and 100 ps are shown. (b) Results for order parameter S^2 0.7 and two fast internal correlation times of 5 and 100 ps are shown. (c) Results for order parameter S^2 0.5 and two fast internal correlation times of 5 and 100 ps are shown.

suitable to derive correlation times around 1 ns, typical for medium-size molecules. The use of the inverse curve (i.e. the $\sigma_{T-ROE}/\sigma_{NOE}$ ratio) may lead

to relevant errors in the region close to $\sigma_{NOE} = 0$, due to its hyperbolic behaviour. In addition, if the relaxation measurements were performed at two different magnetic fields, i.e. 300 and 500 MHz, the differences due to the magnetic field strength for $\sigma_{NOE}/\sigma_{T-ROE}$ ratios are much more evident than those for $\sigma_{NOE}/\sigma_{ROE}$ ratios. Therefore, if only one experiment must be chosen, T-ROESY seems to be at least as adequate as ROESY for medium-size oligosaccharides. These conclusions are basically the same when considering models I–IV on one hand, or model V (regular Lipari–Szabo model-free approach) on the other hand. In model V, there are significant differences in the $\sigma_{NOE}/\sigma_{T-ROE}$ ratio depending on the timescale of the fast motions (5–100 ps). Although also detectable, the variations of $\sigma_{NOE}/\sigma_{ROE}$ ratios with the internal motion rates are much smaller. In any case, when affordable, the use of two magnetic fields [3a] is strongly advisable in order to extract conclusions.

In conclusion, ^1H NMR data have shown that the glycosidic bonds of **1** in solution present distinct flexibility, in contrast with previously reported results for different analogues [10]. From a general point of view, we have demonstrated that the simultaneous recording of NOESY, T-ROESY, and ROESY spectra provides a direct and relatively rapid method to detect the presence of differential motions around the glycosidic linkages of oligosaccharides. In addition, we have shown that it is necessary to treat flexibility in an explicit way in order to obtain a satisfactory agreement between the observed and predicted data. As proposed by Lommersee et al. [15], treatment of internal motion is easily accomplished by using local correlation times for every proton pair within the molecule.

3. Experimental

Molecular mechanics.—Molecular mechanics calculations were performed using the CVFF force field [21] within the DISCOVER program of BIOSYM technologies (San Diego, CA, USA). The chosen structure was built using the Φ/Ψ values reported for the global minima of similar compounds [10] and extensively minimized with conjugate gradients. Intraresidue proton–proton distances were estimated from this structure and employed to calculate the intraresidue cross-relaxation rates. In addition, and although the results should be treated as merely qualitative the obtained interresidue distances were

also measured and employed to calculate the corresponding cross-relaxation rates.

NMR experiments.—NMR experiments were recorded on a Varian Unity 500 spectrometer, using a 10 mmol soln of **1** in 3:1 D₂O:Me₂SO-*d*₆. Selective inversion 1D experiments were performed using the DANTE-Z module [22]. In particular, 1D-NOESY, 1D-ROESY, and 1D-T-ROESY experiments were carried out. NOESY experiments were recorded using mixing times of 100, 200, 400, 600, and 800 ms. ROESY and T-ROESY experiments used mixing times of 100, 200, 300, and 400 ms. The rf carrier frequency for ROESY was set at δ 6.0 ppm, and the spin-locking field was 2.5 kHz. For T-ROESY the carrier was set at the residual water frequency and the spin-locking field was 8.5 kHz. Under these conditions, $\sigma_{\text{T-ROE}}$ is the mean value of σ_{NOE} and σ_{ROE} [13].

The theory under T-ROESY has been discussed by Hwang and Shaka [13], but a brief explanation will be given here: For an isolated pair of protons under isotropic motion with overall correlation time τ_c , the laboratory cross-relaxation rate is given by

$$\sigma_{\text{NOESY}} = (k^2/10)\tau_c[6J(2\omega) - J(0)].$$

On the other hand, the rotating frame cross-relaxation rate is

$$\sigma_{\text{ROESY}} = (k^2/10)\tau_c[2J(0) + 3J(\omega)].$$

An undesirable characteristic of the ROESY experiment is the possibility of net magnetization transfer in *J*-coupled spin systems. This feature complicates the interpretation of ROESY spectra. A modified experiment, called transverse ROESY or just T-ROESY has been proposed recently [13]. Several spin-locking modules have been proposed, and one such sequence consists on the repetitive application of the simple phase-alternating pulse pair $180_x 180_{-x}$. Magnetization, initially along the *y*-axis, is spin-locked on average, allowing measurable enhancement to build up. Near resonance, the net rotation axis is aligned along the *y*-axis of the rotating frame, and, under these conditions, the apparent cross-relaxation rate is given by

$$\sigma_{\text{T-ROESY}} = \frac{1}{2}[(1 + \sin \theta_i \sin \theta_j)\sigma_{\text{ROESY}} + \cos \theta_i \cos \theta_j \sigma_{\text{NOESY}}].$$

If $\theta_i, \theta_j \rightarrow 0$, for strong spin-locking fields,

$$\sigma_{\text{T-ROESY}} = \frac{1}{2}(\sigma_{\text{ROESY}} + \sigma_{\text{NOESY}})$$

which means that this experiment measures the mean of both cross-relaxation rates.

Thus, for large molecules,

$$\sigma_{\text{NOESY}} = -\frac{1}{2}\sigma_{\text{ROESY}}$$

and

$$\sigma_{\text{T-ROESY}} = \frac{1}{4}\sigma_{\text{ROESY}}.$$

For small molecules, there is little difference between ROESY and T-ROESY peak intensities in any event.

The experiments were carried out at 299 K. Cross-relaxation rates [23] were obtained as described [6]. Estimated errors are better than 10%.

In a first step, assuming the spectral density functions of models I–IV (see below), correlation times were estimated from σ ratios, after developing the spectral density functions, $J(n, \omega)$, in function of the correlation time, τ_c , and of the spectrometer frequency, ω_0 . The resultant quartic equation, which exclusively depends on the correlation time of the corresponding proton pair and on the spectrometer frequency, was solved:

$$\frac{\sigma_{\text{NOESY}}}{\sigma_{\text{ROESY}}} = \frac{5 + 22\omega_0^2\tau_c^2 + 8\omega_0^4\tau_c^4}{5 + \omega_0^2\tau_c^2 - 4\omega_0^4\tau_c^4}.$$

The experimental NMR measurements were fitted versus two different motional models based on the Lipari–Szabo model-free approach [16], as described by Lommersee et al. [15]. In particular, models I and III were explored here, although all the reported models [15] are described below.

Model I: Rigid isotropic motion, with only one global correlation time.

$$J(\omega) = \frac{\tau_0}{1 + (\omega\tau_0)^2}.$$

Model II: The spectral density function is modified by assuming different generalized order parameters (S_f^2) for every proton–proton pair. Thus, the global correlation time accounts for the slow motions of the molecule and S_f^2 for the fast internal motions around the glycosidic linkages and/or the monosaccharide rings (first term of the spectral density function within the model-free approach).

$$J(\omega) = S_f^2 \frac{\tau_0}{1 + (\omega\tau_0)^2}.$$

Model III: If the S_f^2 order parameters are not available, it is possible to include fast internal motions by assuming different effective correlation times for every proton pair.

$$J(\omega) = \frac{\tau_{\text{eff}}}{1 + (\omega\tau_{\text{eff}})^2}.$$

Model IV: Both S_f^2 and effective correlation times are used for every proton pair.

$$J(\omega) = S_f^2 \frac{\tau_{\text{eff}}}{1 + (\omega\tau_{\text{eff}})^2}.$$

Model V: The regular Lipari–Szabo model-free approach, where τ_e represent a single effective correlation time describing the internal motions.

$$J(\omega) = \frac{S^2\tau_0}{1 + \omega^2\tau_0^2} + \frac{(1 - S^2)\tau}{1 + \omega^2\tau^2}$$

$$\tau = \tau_0\tau_e / (\tau_0 + \tau_e).$$

When these spectral density functions are included in the equations described above for σ_{NOESY} , σ_{ROESY} , and $\sigma_{\text{T-ROESY}}$, theoretical NOE, ROE, and T-ROE cross-relaxation rates may be calculated. A simple algorithm was used for fitting the experimental data to the different models. Models I and III were chosen, since they do not require accurate order parameters, and they can be used to evaluate the need for distinct correlation times for the different proton pairs. A target function R_w was defined which represent the deviation between the calculated relaxation data and the experimental, with $R_w = 0$ for an exact fit.

$$R_w = \sqrt{\sum_{i=1}^n \frac{(\sigma_{\text{NOE}_i}^{\text{calc}} - \sigma_{\text{NOE}_i}^{\text{exp}})^2 + (\sigma_{\text{ROE}_i}^{\text{calc}} - \sigma_{\text{ROE}_i}^{\text{exp}})^2 + (\sigma_{\text{T-ROE}_i}^{\text{calc}} - \sigma_{\text{T-ROE}_i}^{\text{exp}})^2}{(\sigma_{\text{NOE}_i}^{\text{exp}})^2 + (\sigma_{\text{ROE}_i}^{\text{exp}})^2 + (\sigma_{\text{T-ROE}_i}^{\text{exp}})^2}}.$$

The subscript i represent data for a particular proton pair, and n is the total number of proton pairs with available experimental data.

The fit to the experimental data was done in independent runs for the intraresidue proton pairs (since there are basically no errors in their corresponding average distances), and for the interresidue proton pairs. In this case, the fastest correlation time of the two pyranoid rings involved in the glycosidic linkage was chosen. All the calculations were performed with home-made software which is available from the authors upon request. For the proton experiments, all the experimental cross-relaxation were used as input, along with the average distances estimated from the molecular mechanics calculations.

Acknowledgements

This work has been supported by DGICYT (PB-93-0127) and the Comunidad de Madrid (AE00049/95). We thank Prof. Martín-Lomas and

Dr. Fernández-Mayoralas for their interest and support throughout this work.

References

- [1] L.A. Lasky, *Science*, 258 (1992) 964–969; D.R. Bundle and N.M. Young, *Curr. Opin. Struct. Biol.*, 2 (1992) 666–673.
- [2] S.W. Homans, *Prog. NMR. Spectrosc.*, 22 (1990) 55–86; K. Bock, *Pure Appl. Chem.*, 55 (1983) 605–622; T. Peters, B. Meyer, R. Stuike-Prill, R. Somorjai, and J.-R. Brisson, *Carbohydr. Res.*, 238 (1993) 49–73; H. van Halbeek, *Curr. Opin. Struct. Biol.*, 4 (1994) 697–709; C.A. Bush, *Curr. Opin. Struct. Biol.*, 2 (1992) 655–663; P. de Waard, B.R. Leeftang, J.F.G. Vliegthart, R. Boelens, G. Vuister, and R. Kaptein, *J. Biomol. NMR*, 2 (1992) 211–226; K.G. Rice, P. Wu, L. Brand, and Y.C. Lee, *Curr. Opin. Struct. Biol.*, 3 (1993) 669–674; S.W. Homans and M. Forster, *Glycobiology*, 2 (1992) 143–151; T.J. Rutherford and S.W. Homans, *Biochemistry*, 33 (1994) 9606–9614; T.J. Rutherford, D.C.A. Neville, and S.W. Homans, *Biochemistry*, 34 (1995) 14131–14137.
- [3a] M. Hricovini, R.N. Shah, and J.P. Carver, *Biochemistry*, 31 (1992) 10018–10023.
- [3b] T.J. Rutherford, J. Partridge, C.T. Weller, and S.W. Homans, *Biochemistry*, 32 (1993) 12715–12724; M. Hricovini and G. Torri, *Carbohydr. Res.*, 268 (1995) 159–175; B.J. Hardy, W. Egan, and G. Widmalm, *Int. J. Biol. Macromol.*, 17–18 (1995) 149–160; P.J. Hajduk, D.A. Horita, and L. Lerner, *J. Am. Chem. Soc.*, 115 (1993) 9196–9201.
- [4] R.U. Lemieux, *Chem. Soc. Rev.*, 18 (1989) 347–374; R.U. Lemieux, K. Bock, L.T.J. Delbaere, S. Koto, and V.S. Rao, *Can. J. Chem.*, 58 (1980) 631–653.
- [5] J.P. Carver, *Pure Appl. Chem.*, 65 (1993) 763–770; T. Peters and T. Weimar, *J. Biomol. NMR*, 4 (1994) 97–116; A. Poveda, J.L. Asensio, M. Martin-Pastor, and J. Jimenez-Barbero, *Chem. Comm.*, (1996) 421–422; C.J. Edge, U.C. Singh, R. Bazzo, G.L. Taylor, R.A. Dwek, and T.W. Rademacher, *Biochemistry*, 29 (1990) 1971–1974; D.A. Cumming and J.P. Carver, *Biochemistry*, 26 (1987) 6664–6676; B.R. Leeftang and L.M.J. Kroon-Batenburg, *J. Biomol. NMR*, 2 (1992) 495–518.
- [6] L. Poppe and H. van Halbeek, *J. Am. Chem. Soc.*, 114 (1992) 1092–1094.
- [7] C. Meyer, S. Perez, C. Herve du Penhoat, and V. Michon, *J. Am. Chem. Soc.*, 115 (1993) 10300; I. Braccini, V. Michon, C. Herve du Penhoat, A. Imbert, and S. Perez, *Int. J. Biol. Macromol.*, 15 (1993) 52–55; J. Dabrowski, T. Kozar, H. Grosskurth, and N.E. Nifant'ev, *J. Am. Chem. Soc.*, 117 (1995) 5534–5539.
- [8] L. Maler, G. Widmalm, and J. Kowalewski, *J. Biomol. NMR*, 7 (1996) 1–7.
- [9] S.B. Engelsen, C. Herve du Penhoat, and S. Perez, *J. Phys. Chem.* 99 (1995) 13334–13351.

- [10] Y. Ichikawa, Y.-C. Lin, D.P. Dumas, G.-J. Shen, E. Garcia-Junceda, M.A. Williams, R. Bayer, C. Ketcham, L.E. Walker, J.C. Paulson, and C.-H. Wong, *J. Am. Chem. Soc.*, 114 (1992) 9283–9298; G.E. Ball, R.A. O'Neil, J.E. Schultz, J.B. Lowe, B.W. Weston, J.O. Nagy, E.G. Brown, C.J. Hobbs, and M.D. Bednarski, *J. Am. Chem. Soc.*, 114 (1992) 5449–5451; C. Mukhopadhyay, K.E. Miller, and C.A. Bush, *Biopolymers*, 34 (1994) 21–29; T.J. Rutherford, D.G. Spackman, P.J. Simpson, and S.W. Homans, *Glycobiology*, 4 (1994) 59–68; J. Breg, L.M.J. Kroon-Batenburg, G. Strecker, J. Montreuil, and J.F.G. Vliegthart, *Eur. J. Biochem.*, 178 (1989) 727–739.
- [11] F.F. Santos-Benito, A. Fernández-Mayoralas, M. Martín-Lomas, and M. Nieto-Sampedro, *J. Exp. Med.*, 176 (1992) 915–919; K. Singh, A. Fernández-Mayoralas, and M. Martín-Lomas, *J. Chem. Soc., Chem. Commun.*, (1994) 775–776.
- [12] J.M. Coterón, K. Singh, J.L. Asensio, M.D. Dalda, A. Fernández-Mayoralas, J. Jiménez-Barbero, and M. Martín-Lomas, *J. Org. Chem.*, 60 (1995) 1502–1513.
- [13] T.L. Hwang and A.J. Shaka, *J. Am. Chem. Soc.*, 114 (1992) 3157–3159.
- [14] D.G. Davis, *J. Am. Chem. Soc.*, 109 (1987) 3471–3472.
- [15] J.P.M. Lommerse, L.M.J. Kroon-Batenburg, J. Kron, J.P. Kamerling, and J.F.G. Vliegthart, *J. Biomol. NMR*, 5 (1995) 79–94.
- [16] G. Lipari and A. Szabo, *J. Am. Chem. Soc.*, 104 (1982) 4546–4559.
- [17] C. Gonzalez, J.A.C. Rullman, R. Boelens, and R. Kaptein, *J. Magn. Reson.*, 91 (1991) 659–664.
- [18] A. Ejchart, J. Dabrowski, and C.-W. von der Lieth, *Magn. Res. Chem.*, 30 (1992) S105–S114; A. Ejchart and J. Dabrowski, *Magn. Res. Chem.*, 30 (1992) S115–S124.
- [19] A. Bax and D.G. Davis, *J. Magn. Reson.*, 63 (1985) 207–213.
- [20] A.A. Bothner-By, R.L. Stephens, J.M. Lee, C.D. Warren, and R.W. Jeanloz, *J. Am. Chem. Soc.*, 106 (1984) 811–813.
- [21] A.T. Hagler, S. Lifson, and P. Dauber, *J. Am. Chem. Soc.*, 101 (1979) 5122–5130.
- [22] D. Boudot, D. Canet, J. Brondeau, and J.C. Boubel, *J. Magn. Res.*, 83 (1989) 428–433.
- [23] D. Neuhaus and M.P. Williamson, *The Nuclear Overhauser Effect in Structural and Conformational Analysis*, VCH, New York, 1989.